Hydrothermal Growth of Single Crystals of TMA-CuGS-2, $[C_4H_{12}N]_6[(Cu_{0.44}Ge_{0.56}S_{2.23})_4(Ge_4S_8)_3]$ and Their Characterization Using Synchrotron/Imaging Plate Data

Kemin Tan,[†] Younghee Ko,[†] John B. Parise,*[,†,‡] and Alex Darovsky[§]

Department of Earth and Space Sciences, State University of New York, Stony Brook, New York 11794; Department of Chemistry, State University of New York, Stony Brook, New York 11794; and SUNY X3 Beamline, National Synchrotron Light Source, Brookhaven National Laboratory, Upton, New York 11973

Received August 9, 1995. Revised Manuscript Received October 25, 1995[⊗]

Single crystals of TMA-CuGS-2, $[C_4H_{12}N]_6[(Cu_{0.44}Ge_{0.56}S_{2.23})_4(Ge_4S_8)_3]$, were synthesized hydrothermally, and the structure was determined using data collected from sealed-tube and synchrotron X-ray sources. This compound consists of $Ge_4S_{10}^{4-}$ adamantine clusters, corner-sharing with MS_x units (M = Cu, Ge; $x = 3$ or 4), forming an open framework with tetramethylammonium cations residing within four intersecting channels. Disorder in the M sites causes the composition of the framework to deviate from the ideal stoichiometry, $Ge_{0.71}M_{0.24}S_2$, realized when M = Cu and $x = 4$. This is consistent with results obtained from electron-probe microanalysis. The structure refinements were carried out in space group $I\bar{4}3d$ with cell parameter $a = 20.629$ (1) Å. Fourteen unique weak reflections of the type hhl, $2h + l = 4n + 2$, forbidden in $I\bar{4}3d$, were detected only in the synchrotron/imaging plate experiment. Trial refinements in space groups $R3$ and $I2_13$ suggest their origin in either weak ordering or multiple scattering effects.

Introduction

Hydrothermal recrystallization of simple metals Sn[1−6], Ge,[7,8] and Sb[9−14] chalcogenides[15] in the presence of organic amines or alkali metals resulted in new families of open-framework materials. Although the crystal structures of some of these have been determined, progress on the characterization of many of these metastable materials is hampered by a lack of samples suitable for conventional single-crystal diffractometry. Pseudosymmetry is also common among certain members of this class of materials. In the germanium sulfide system, for example, a series of compounds of one structural type, such as TMA-MGS-2 (TMA: tetramethylammonium), can be obtained by using different transition metals (M) while keeping other synthetic conditions unchanged.[1] Similarities in the X-ray powder diffraction patterns for members of the GS-2-family supports the conclusion that one structure model is enough to describe every compound in the series. However, variety in the stereochemistry of the transition metals coordinating sulfur[16] could lead to subtle structural modifications. These fine details of structure, which could bear on the chemistry of the systems involved, are best studied using single-crystal rather than, for example, powder diffraction techniques.

TMA-CuGS-2 was one of the TMA-MGS-2 type compounds reported in the patent literature.[1] Its powder diffraction pattern is similar to that of TMA-CoMnGS-2.[1,7] This compound (Figure 1) crystallizes as a framework consisting of two building units, 4-connected $Ge_4S_{10}^{4-}$ adamantine and 3-connected MS_4 (M = Mn/Co) clusters.[7] Each $Ge_4S_{10}^{4-}$ is corner-sharing only with MS_4 and vice versa, forming a (3,4)-connected open framework. The composition of this framework is $3 \times (Ge_4S_8) + 4 \times (MS_{2.5}) = Ge_{12}M_4S_{34}$, which normalizes to $Ge_{0.71}M_{0.24}S_2$ (possible protons attached to the framework are neglected). If TMA-CuGS-2 were isostructural with TMA-MnCoGS-2, the framework should be consistent with this composition. Instead the chemical analysis reported for the CuGS-2 material is $Ge_{0.89}Cu_{0.11}S_2$.[1] In this paper, we report the hydrothermal synthesis, composition, and structural analysis of TMA-CuGS-2 single crystals. For structural studies, besides conventional single-crystal diffractometry, synchrotron radiation in combination with an imaging plate (IP)

[†] Department of Earth and Space Sciences, SUNY.
[‡] Department of Chemistry, SUNY.
[§] Brookhaven National Laboratory.
[⊗] Abstract published in *Advance ACS Abstracts,* December 1, 1995.

(1) Bedard, R. L.; Vail, L. D.; Wilson, S. T.; Flanigen, E. M. U.S. Patent 4,880,761, 1989.
(2) Parise, J. B.; Ko, Y.; Rijssenbeek, J.; Nellis, D. M.; Tan, K.; Koch, S. *J. Chem. Soc., Chem. Commun.* **1994**, 527 and references therein.
(3) Parise, J. B.; Ko, Y. *Chem. Mater.* **1994**, *6*, 718−720.
(4) Parise, J. B.; Ko, Y.; Tan, K.; Nellis, D. M.; Koch, S. *J. Solid State Chem.* **1995**, *117*, 219−228.
(5) Jiang, T.; Ozin, G. A.; Bedard, R. L. *Adv. Mater.* **1994**, *6*, 860−865.
(6) Tan, K.; Ko, Y.; Parise, J. B. *Acta Crystallogr.* **1995**, *C51*, 398−401.
(7) Bedard, R. L.; Wilson, S. T.; Vail, L. D.; Bennett, J. M.; Flanigen, E. M. In *Zeolites: Facts, Figures, Future. Proceedings of the 8th International Zeolite Conference*; Jacobs, P. A., Santen, R. A. v., Ed.; Elsevier: Amsterdam, 1989; pp 375−387.
(8) Tan, K.; Darovsky, A.; Parise, J. B. *J. Am. Chem. Soc.* **1995**, *117*, 7039−7040 and references therein.
(9) Parise, J. B. *J. Chem. Soc., Chem. Commun.* **1990**, 1553−1554.
(10) Parise, J. B. *Science* **1991**, *251*, 293−294.
(11) Parise, J. B.; Ko, Y. *Chem. Mater.* **1992**, *4*, 1446−1450.
(12) Ko, Y.; Cahill, C.; Parise, J. B. *J. Chem. Soc., Chem. Commun.* **1994**, 69−70.
(13) Tan, K.; Ko, Y.; Parise, J. B. *Acta Crystallogr.* **1994**, *C50*, 1439−1442.
(14) Wang, X.; Liebau, F. *J. Solid State Chem.* **1994**, 385−389.
(15) Barrer, R. M. *Hydrothermal Chemistry of Zeolites*; Academic Press: London, 1982.
(16) Vaughan, D. J.; Craig, J. R. *Mineral Chemistry of Metal Sulfides*; Cambridge University Press: Cambridge, 1978.

0897-4756/96/2808-0448$12.00/0

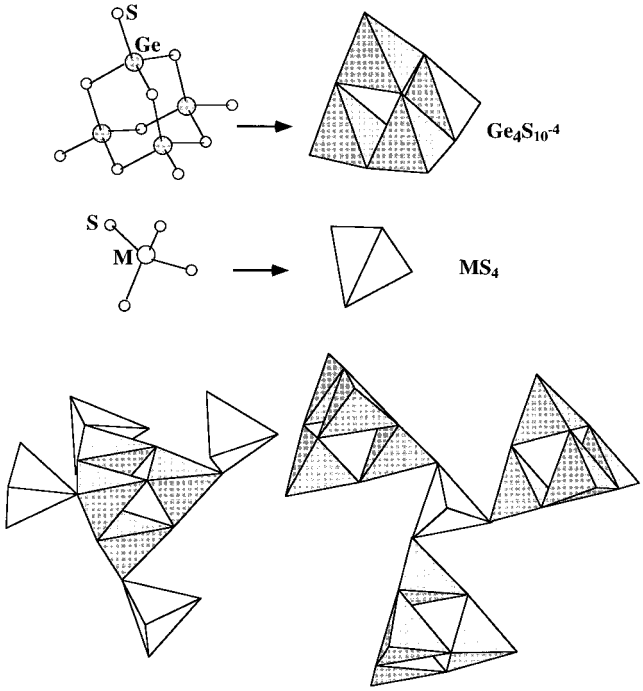

Figure 1. Building units and their connections in TMA-CoMnGS-2 and TMA-CuGS-2 structures. The 4-connected $Ge_4S_{10}^{4-}$ adamantine clusters are only corner-sharing with the 3-connected MS_4 motifs and vice versa. In the TMA-CuGS-2 structure, the 3-connected motifs are a mixture of MS_3 and MS_4.

detection system was employed. The greater dynamic range and sensitivity afforded by the synchrotron/IP system was important for the detection of subtle diffraction phenomena not observed with conventional diffraction techniques. This technology, adapted from the protein crystallographic community,[17] has proved to be very successful in the structure analysis of small inorganic crystals, especially those with open frameworks.[8,18]

Experimental Section

Synthesis and Characterization. Freshly precipitated amorphous GeS_2 (0.2 g), $[TMA]HCO_3$ solution (0.6 mL, prepared by bubbling CO_2 through 40% [TMA]OH until pH = 9.7), $Cu(CH_3COO)_2 \cdot H_2O$ (0.03 g) and [TMA]Cl (0.044 g) were combined. The resulting slurry was heated at 150 °C under autogenous hydrothermal conditions in a Pyrex-lined bomb for 1 day. Tris-tetrahedral[19] single crystals up to 200 μm on edge were obtained with 90% yield based on GeS_2.

Electron-probe microanalysis (EPMA) was carried out using a Cameca Camebax instrument. The accelerating voltage was set to 15 kV and the beam current 10 nA. To minimize beam damage, a rastered beam of 20 μm was used. The quantitative compositional analysis, summarized in Table 1, is consistent with the formulation $Ge_{0.82}M_{0.10}S_2$ for the framework. This accords with the composition given in the literature, $Ge_{0.89}Cu_{0.11}S_2$,[1] clearly showing the deviation from $Ge_{0.71}M_{0.24}S_2$, calculated assuming Ge occupies only metal sites in the adamantine clusters in the structure (Figure 1). An accurate analysis is particularly important in those cases where site occupancy disorder is suspected.

Thermogravimetric analysis (TGA) was conducted using a Perkin-Elmer thermal analysis system. A 8.227 mg sample was heated under nitrogen at the rate of 2.0 °C/min from room temperature to 400 °C. A 17.7% weight loss was observed between 250 and 350 °C. This loss is consistent with the EPMA data, which suggest an average of 18.3 wt % of the TMA-CuGS-2 sample consists of volatile components (see Table 1).

Preliminary X-ray Study and Structure Analysis. A crystal 150 μm on edge was studied using precession photography and it indicated a body-centered cubic lattice with Laue class $m\bar{3}m$. The X-ray powder diffraction pattern, reproduced in Figure 2, included all peaks of TMA-CuGS-2 reported in the patent literature[1] and, with the exception of one peak, can be indexed with a body-centered cubic cell with $a = 20.629(1)$ Å. The extra peak was located at $2\theta = 15.467°$ and was attributed to germanium sulfide (JCPDS entry 270238),[20] which recrystallized as a byproduct of the amorphous starting material (GeS_2) during the hydrothermal synthesis. A peak, located at $2\theta = 25.993°$ and indexed as (442, 600), should be absent in the space group $I\bar{4}3d$ determined in the experiments described later. However, the indexing of the peak was uncertain because of overlap with the major peak of GeO_2 (JCPDS entry 361463),[20] a common impurity.[1,8] Several other weak peaks due to GeO_2 are discernible above background at $2\theta = 20.5$, 38.13, and 41.6° (Figure 2).

A set of single-crystal X-ray diffraction data was collected on a Picker four-circle diffractometer (sealed tube, Mo Kα, 50 kV and 20 mA). The structure was then solved in space group $I\bar{4}3d$ using the direct methods routines in Shelxs-86.[21] The subsequent refinements were carried out by using a package of programs written and maintained by Calabrese.[22] The structure is related to TMA-MnCoGS-2,[7] which was reported in the subgroup $R3$. Fourier difference synthesis revealed the transition metal (M) site, assigned to Cu in the initial structural model of TMA-CuGS-2, was split as shown in Figure 3. To describe the disordering of the M-site more precisely and to investigate the possible pseudosymmetry,[7] a synchrotron/imaging plate experiment was undertaken.

Synchrotron/Imaging Plate Experiment. A tris-tetrahedral crystal, 40 μm in diameter and with less mosaicity than the large crystal used in the preliminary experiments, was mounted atop a glass fiber 20 μm in diameter and analyzed at the X-3 beamline of the National Synchrotron Light Source (NSLS). The smaller crystal reduces the effects of extinction and absorption. A set of 30 reflections in the range $12° < 2\theta < 39°$ was measured with a scintillation counter to obtain a precise orientation matrix. To collect intensity data, an image plate cassette was mounted on the detector arm replacing the scintillation counter. Data were collected as described previously[8] and are given in Table 2. The orientation matrix was used to index reflections on the imaging plates. After each image was processed to obtain the refined crystal-to-plate distance and the IP tilt angles,[23] a total of 11 677 fully recorded reflections with $I > 1.0\sigma(I)$ were integrated using the "seed-skewness" method.[24] Those reflections close to the oscillation axis, IP margins, or oscillation boundaries were rejected.

Results and Discussion

Space Group. The data obtained were consistent with a cubic cell. Using the program SORTAV,[25] reflections were merged in point group $\bar{4}3m$ with R_{merge} of 5.6%, based on intensity. This resulted in 1186

(17) (a) Miyahara, J.; Takahashi, K.; Amemiya, Y.; Kamiya, N.; Satow, Y. *Nucl. Instrum. Meth.* **1986**, *A246*, 572−578. (b) Hajdu, J.; Machin, P. A.; Campbell, J. W.; Greenhough, T. J.; Clifton, I. J.; Zurek, S.; Gover, S.; Johnson, L. N.; Elder, M., *Nature*, **1987**, *329*, 178−181. (c) Sakabe, N. *Nucl. Instrum. Meth.* **1991**, *303*, 448−463.

(18) Ko, Y.; Tan, K.; Parise, J. B.; Darovsky, A., manuscript in preparation.

(19) (a) A tris-tetrahedral crystal consists of 12 faces; each of the four tetrahedral faces is terminated by three (tris) additional faces. (b) Klein, C.; Hurlbut, Jr. C. S. *Manual of Mineralogy*; John Wiley & Sons: New York, 1985.

(20) *JCPDS Powder Diffraction File-Inorganic Phases*; International Centre for Diffraction Data: 1601 Park Lane, Swarthmore, PA 19081-2389, 1988.

(21) Sheldrick, G. M. *Acta Crystallogr.* **1990**, *A46*, 467−473.

(22) Calabrese, J. C. The Z package of programs, EI DuPont, Wilmington, DE.

(23) Bolotovsky, R. The IPMS program, Chemistry Department, State University of New York, Buffalo, NY.

(24) Bolotovsky, R.; White, M. A.; Darovsky, A.; Coppens, P. *J. Appl. Cryst.* **1994**, *28*, 86−95.

Table 1. Compositions of TMA-CuGS-2 Single Crystals (Element Weight Percentages by Electron Probe Microanalysis)

sample[a]	CGS-1 1	CGS-1 2	CGS-2 1	CGS-3 1	CGS-4 1	CGS-2 2	CGS-3 2	CGS-4 2	av
measurement									
Ge, %	37.72	37.95	38.28	37.62	36.77	37.67	36.51	37.38	37.49(59)
Cu, %	4.37	3.61	4.61	3.73	4.74	4.03	3.57	3.38	4.01(51)
S, %	40.39	40.57	40.87	40.55	39.54	40.62	39.40	40.59	40.32(29)
others, %	17.52	17.87	16.24	18.10	18.95	18.76	20.52	18.65	18.3(1.3)
atomic fraction (normalized to S_2)	$Ge_{0.83}Cu_{0.11}$	$Ge_{0.83}Cu_{0.09}$	$Ge_{0.83}Cu_{0.11}$	$Ge_{0.82}Cu_{0.09}$	$Ge_{0.82}Cu_{0.12}$	$Ge_{0.82}Cu_{0.10}$	$Ge_{0.82}Cu_{0.09}$	$Ge_{0.81}Cu_{0.08}$	$Ge_{0.82}Cu_{0.10}$

[a] CGS-1 etc. are labels for experimental crystals. 1 etc. are sequence numbers of experiments on one crystal. In the first five measurements, chalcopyrite, $CuFeS_2$, was used as the standard for Cu and S; Ge metal as the standard for Ge. In the last three measurements, Cu metal instead of chalcopyrite was used as the standard for Cu. The four sample crystals were from the same batch as those used in the X-ray diffraction experiments.

unique data; of these 97 were measured only once, 44 were merged from two symmetry-equivalent reflections, and the remainder were merged from three or more individuals. Percentages of the unique reflections measured with $I > 1.0\sigma(I)$ in equal-volume intervals are shown in Figure 4. The intensity distribution of equivalent reflections showed no systematic deviation from $\bar{4}3m$ symmetry, with no obvious groupings suggestive of either 23- or 3-point group symmetry. As an example, the intensities of $(97\bar{6})$ and its equivalents were listed in order of ascending intensity in Table 3. Using the known structure model obtained from the data set collected on the Picker diffractometer, the refinement in space group $I\bar{4}3d$ quickly converged with $R = 4.96\%$ and $R_w = 2.76\%$ (Table 2).

Among the 11 677 integrated intensities, there were 34 violating the extinction rule hhl, $2h + l = 4n \pm 2$) for space group $I\bar{4}3d$. These reflections were distributed over 25 imaging plates and were some 500 times weaker than the strongest observed. The symmetry equivalents and Friedel pairs of some of them (e.g., 554, 778, and 994) were detected, and this set of reflections was merged into 14 uniques, including five Friedel pairs. The presence of this group of reflections suggests a possible lower-symmetry space group, $I2_13$ or $R3$. The relationships between these subgroups and supergroup $I\bar{4}3d$ is

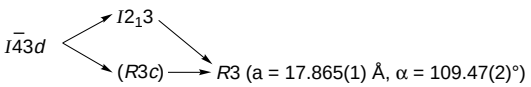

Refinements were carried out in the subgroups to see if (a) the M-site splitting in $I\bar{4}3d$ results in ordering in a lower-symmetry group and (b) the calculated intensities of those "forbidden" reflections match the experimental data in either $I2_13$ or $R3$. The values of R_{merge} for these space groups were approximately 4% based upon intensity. The structures were solved in each of the trial space groups, and the atomic coordinates and displacement parameters refined to convergence. The structural features, for example, the split M site and the displacement parameters of the neighboring sulfur sites, were the same as in $I\bar{4}3d$. The positions of crystallographically unique atoms, in space group $R3$, for example, were related within 3σ to others in the atom list through the symmetry operators removed from $I\bar{4}3d$. In both space groups $I2_13$ and $R3$, the calculated intensities of the reflections forbidden in $I\bar{4}3d$ were systematically weaker than those observed. This was the case for all refinements starting from a variety of atomic positions.

The results of these preliminary refinements in the lower symmetry groups imply these weak "forbidden" reflections originated from either distortions or order-

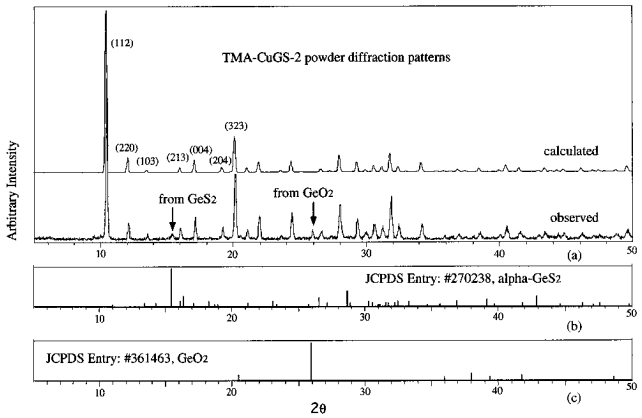

Figure 2. Measured and calculated powder diffraction patterns of TMA-CuGS-2 (a). The powder diffraction experiment was performed on a Scintag diffractometer using Cu Kα radiation. The powder diffraction patterns of α-GeS_2 (b) and GeO_2 (c) from JCPDS.[20]

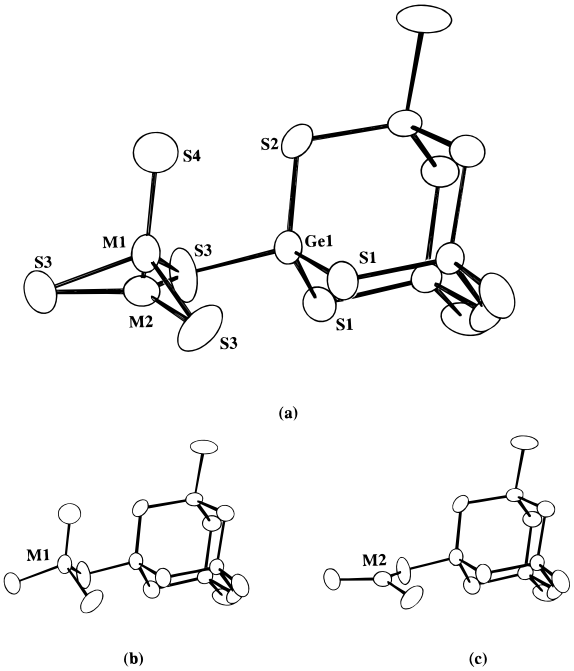

Figure 3. (a) Site of the M atom in the TMA-CuGS-2 structure splits into M1 and M2, showing two stereochemistries for the metal atom. (b) M1 is 4-coordinated while (c) M2 is 3-coordinated. The displacement ellipsoids in these ORTEP[31] drawings are scaled to enclose 50% probability.

(25) Blessing, R. H. *J. Appl. Cryst.* **1989**, *22*, 396−397 and references therein.

Table 2. Selected Crystallographic Data for the Synchrotron/Imaging Plate Experiment

Crystal Data	
unit-cell contents	$[C_4H_{12}N]_6[(Cu_{0.44}Ge_{0.56}S_{2.23})_4(Ge_4S_8)_3]$
chemical formula wt	2647.1
crystal system	cubic
space group	$I\bar{4}3d$
unit cell	$a = 20.629(1)$ Å
vol of unit cell	8779(1) Å^3
formula per unit cell Z	4
density calculated from formula and cell	2.002 g/cm^3
radiation type and wavelength	synchrotron, $\lambda = 0.642$ Å
no. of reflns for cell meast and 2θ range	30 reflections, $12 < 2\theta < 39°$
meast temp	room temp
crystal shape, color, and size	tris-tetrahedron, reddish-yellow, 0.04 mm on edge
Data Collection	
data-collection method	imaging plate
crystal-to-imaging plate distance	150 mm
exposure time	3 min and gradually increased with the decay of the beam intensity
imaging plate	Fuji imaging plate, medical, high resolution, HR-V, 20 × 25 cm
scanner	Fujix, bioimaging analyzer, BAS2000
gradation	1024
latitude	4
resolution	100 μm
sensitivity	10000
oscillation angle	5°
overlap angle	2°
ϕ range	185°
no. of images	60
no. of reflns integrated ($I > 1.0\sigma(I)$)	11 677
no. of independent reflections	1186
merge R	0.056
min, max, value of θ	5.23°, 29.54°
absorption correction	no
Refinement	
refinement on	F
final R and R_w	0.0485, 0.0269
S	1.40
no. of parameters refined	49
no. of reflection used	1075 ($\theta_{max} = 25.4°$)
weighting scheme	$w = [\sigma^2(I) + 0.0009I^2]^{-1/2}$
max (Δ/σ)	0.01
max residual electron density	0.83 e Å^{-3}

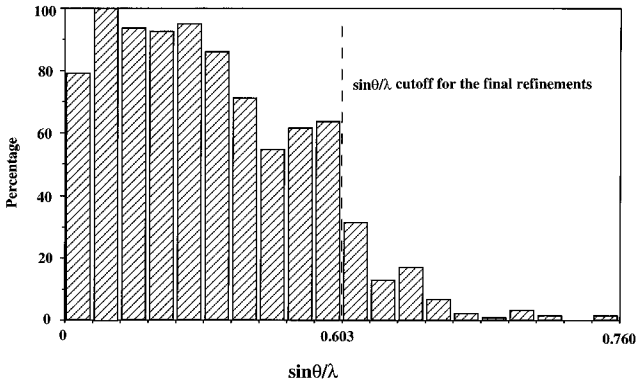

Figure 4. Percentages of unique reflection measured with $I > 1.0\sigma(I)$ in equal-volume shells of $s = \sin\theta/\lambda$. Each volume is approximately 0.7356 Å^{-3}. The number at higher angle was limited by the flat-plate geometry of the detection system. Some lower angle reflections were blocked by the beam stop.

ings, not resolved in this study, or from some effects unrelated to the choice of space group. Possibilities for the later include Renninger effects.[26] The short wave length (0.642(1) Å) and large unit cell ($V = 8779(1)$ Å^3) produced a dense reciprocal lattice, greatly increasing the possibility of multiple scattering. While this study concentrates on the hydrothermal synthesis, composition, and average structure of TMA-CuGS-2, further characterization of these weak reflections and the study of other compounds in this series will be reported elsewhere. For this report, all subsequent discussion of the structure of TMA-CuGS-2 refers to space group $I\bar{4}3d$.

Final Structural Refinements. The crystallographic model consistent with the IP and EPMA data, along with the geometric results calculated from it, are summarized in Tables 4 and 5. As shown in Figure 3, two sites, M1 and M2 about 0.835 Å apart, are resolved as the link between the $Ge_4S_{10}^{4-}$ adamantine clusters. The model implies two stereochemistries (Figure 3b,c) for the metal connection; one in 4-fold and the other in 3-fold coordination with sulfur. The M1 and M2 sites lie on the 3-fold axis perpendicular to the trigonal plane formed by the three neighboring S atoms, labeled S3 in Figure 3. The displacement ellipsoids of the these S atoms were elongated and tilted away from the axis. Their equivalent isotropic displacement parameters (B_{eq}) are about 25−45% larger (Table 4) than those bonded to the Ge atoms, indicative of static disorder in the S3 sites related to partial occupancy of neighboring M sites.

Refinements were undertaken in an attempt to determine the types of atoms on the M sites. When both sites were constrained to contain only Cu, their refined isotropic displacement parameters were smaller than those of Ge atoms within the adamantine clusters (Figure 3). Occupancy of the M sites by Cu alone is

(26) Renninger, M. *Z. Physik* **1937**, *106*, 141.

Table 3. Intensities of (97$\bar{6}$) Reflection and Its Equivalents Ordered with Increasing Intensity

h	*k*	*l*	*I*	$\sigma(I)$	no. of IP	S^a	$\sigma(S)$
−7	9	6	28 039.63	754.87	42	0.989	0.006
−9	6	7	28 743.24	787.56	48	0.993	0.007
−9	6	7	29 371.33	838.22	47	1.102	0.008
6	7	−9	29 544.90	778.52	11	1.067	0.007
6	9	−7	29 564.83	918.06	14	1.056	0.007
−9	7	6	29 864.52	727.07	46	0.992	0.007
9	7	−6	30 291.73	904.95	9	1.055	0.006
−6	7	9	30 383.33	785.43	45	0.998	0.007
7	6	−9	30 544.52	925.22	9	1.055	0.006
9	6	−7	30 570.62	899.27	8	1.047	0.007
−7	6	9	30 637.73	790.60	47	1.102	0.008
−6	9	7	30 786.90	814.75	41	1.000	0.000
7	9	−6	30 864.29	934.87	13	1.105	0.007
9	6	−7	31 205.09	869.75	7	1.061	0.008
9	−6	7	32 580.22	783.67	31	0.953	0.006
av			29 851.97	831.06			

[a] *S*, the refined scaling factor of intensity for each imaging plate.

Table 4. Fractional Coordinates ($\times 10^4$) and Isotropic Displacement Parameters (Å^2) for TMA-CuGS-2

atom	site/occupancy	*x*	*y*	*z*	B_{eq}/B_{iso}[a]
Ge(1)	48*e*/1.0	6675.1(4)	5644.9(4)	10201.1(4)	3.2(1)
M1[b]	16*c*/0.73	5358(1)	4642(1)	9642(1)	3.5(1)
M2[c]	16*c*/0.27	5125(1)	4875(1)	9875(1)	3.8(1)
S(1)	48*e*/1.0	6424(1)	6236(1)	9339(1)	3.9(1)
S(2)	24*d*/1.0	7500	4991(1)	10000	4.5(1)
S(3)	48*e*/1.0	5846(1)	5076(1)	10528(1)	5.7(1)
S(4)	16*c*/0.73	5962(1)	4038(1)	9038(1)	6.2(1)
N(1)	24*d*/1.0	7500	2837(7)	10000	9.5(4)
C(1)[d]	48*e*/1.0	6946(11)	2377(13)	9724(9)	20.5(7)
C(2)	48*e*/1.0	7754(6)	3254(7)	9467(6)	10.6(3)

[a] B_{iso} for N(1) to C(2); $B_{eq} = (8\pi^2/3)\sum_i\sum_j U_{ij} a_i^* a_j^* \boldsymbol{a_i}\cdot\boldsymbol{a_j}$ for others. [b] The scattering in the M-1 site was assigned to Ge in the final refinements. [c] The scattering in the M-2 site was assigned to Cu in the final refinements. [d] The relatively large B_{iso} of C(1) atom might indicate some degree of static disorder.

Table 5. Selected Interatomic Distances (Å) and Angles (deg)[a]

Ge(1)−S(1)	2.223(2)	S(1)−Ge(1)−S(1)[a]	111.62(5)
Ge(1)−S(1)[a]	2.240(2)	S(1)−Ge(1)−S(2)	111.39(6)
Ge(1)−S(2)	2.215(2)	S(1)[a]−Ge(1)−S(2)	112.56(7)
Ge(1)−S(3)	2.184(2)	S(1)[a]−Ge(1)−S(3)	100.14(8)
M1−S(3)	2.275(2)	S(1)−Ge(1)−S(3)	111.2(1)
M1−S(4)	2.162(1)	S(2)−Ge(1)−S(3)	109.45(9)
M2−S(3)	2.053(2)	S(3)−M1−S(3)[d]	102.41(8)
		S(3)−M1−S(4)	115.85(6)
M1−M2[b]	0.8346(1)	S(3)−M2−S(3)[d]	119.42(2)
		Ge(1)−S(1)−Ge(1)[b]	104.3(1)
		Ge(1)−S(2)−Ge(1)[c]	104.8(1)
		Ge(1)−S(3)−M1	108.1(1)
		Ge(1)−S(3)−M2	118.4(1)

[a] Symmetry operation codes: (*a*) $-^1/_4 + z$, $^5/_4 - y$, $^7/_4 - x$; (*b*) $^7/_4 - z$, $^5/_4 - y$, $^1/_4 + x$; (*c*) $^3/_2 - x$, *y*, $2 - z$; (*d*) $1 - y$, $-^1/_2 + z$, $^3/_2 - x$. [b] The distance between two partially occupied sites; occupancies fixed to sum to 1.0.

Table 6. Isotropic Displacement Parameters and Discrepancy Indices with M1 Site Assigned to Cu (Top) and Ge (Bottom)[d]

	Ge(1)	M1[a]	M2	S(1)	S(2)	S(3)	S(4)	*R*	*Rw*
M1:Cu[b]	3.2(1)	2.8(1)	3.0(1)	4.0(1)	4.6(1)	5.8(1)	6.7(1)	4.96%	2.76%
M1:Ge[c]	3.2(1)	3.5(1)	3.8(1)	3.9(1)	4.5(1)	5.7(1)	6.2(1)	4.85%	2.69%

[a] The sum of the site occupancy factor (SOF) of the M1 and M2 is unity. The SOF of S(4) equals that for M1. See Tables 4 and 5 for positional parameters of sites. [b] Isotropic displacement parameters when only Cu occupies M1 site with SOF 0.75 and Cu in M2 with SOF = 0.25. [c] Isotropic displacement parameters when only Ge occupies M1 site with SOF = 0.73 and Cu in M2 with SOF = 0.27. [d] $B_{eq} = (8\pi^2/3)\sum_i\sum_j U_{ij} a_i^* a_j^* \boldsymbol{a_i}\cdot\boldsymbol{a_j}$, Å^2.

inconsistent with the chemical analysis and the refined displacement parameters (Table 6) suggested partial occupancy by an element of higher atomic number. Simple crystal chemistry[27] argues for occupancy of the 3-coordinated M2 site by Cu and that the 4-coordinated M1-site is occupied by a combination of Cu and Ge consistent with the chemical analysis. Fortunately, the scattering factors of Cu and Ge are sufficiently close to allow determination of the relative scattering power of the two M sites from constrained refinement, where both sites are occupied by the same element and their displacement parameters are fixed. Having determined the relative occupancy, the Cu was partitioned into the M2 site and the remaining Cu and Ge into the M1 site. The EPMA experiments indicated the ratio of Cu to Ge for this sample of TMA-CuGS-2 is 0.10:0.82 (Table 1). On the basis of this information, it was estimated that 23% of the atoms occupying the M1 sites are Cu and that the remainder are Ge, giving a calculated composition of the framework, $Ge_{0.87}Cu_{0.11}S_2$. This normalized atomic fraction is close to the average composition determined in the chemical analysis (Tables 1 and 7).

Although the oxidation states of Cu in the M1 and M2 sites are not addressed directly in this study, they are likely to be +2 and +1, respectively.[16,27,28] Three-coordinated Cu^{2+}, while rare in mineral sulfides,[16] is well characterized in both the (I) and (II) formal valence states in the mineral covellite (CuS).[16,29] However, the three Cu(II)−S bonds are shorter than expected from those found in covellite,[29] 2.05 Å rather than 2.19 Å; this is attributed to the static disordering of S(3) sites. The refined position of the S(3) site actually represents the weighted average value of the two S(3) positions coordinated to the M1 and M2 sites. For the same reason, the Cu(I)−S bond length for Cu occupying the 4-coordinated M1 site, is shorter than found for CuS,

(27) Slupecki, O.; Brown, I. D. *Acta Cryst.* **1982**, *B38*, 1078−1079.
(28) Cotton, F. A.; Wilkinson, G. *Advanced Inorganic Chemistry*; John Wiley & Sons: New York, 1988.
(29) Berry, L. G. *Am. Mineral.* **1954**, *39*, 504−509.

Table 7. Comparison of the Calculated Compositions of TMA-CuGS-2, Determined from Different Structural Models, with Chemical Analysis

	model 1: M site is fully occupied by Cu[a]	model 2: M site is coocupied by Cu and Ge[b]	EPMA[c] on single-crystal samples	chemical analysis on powder sample[1]
Ge, %	33.11	39.06	37.49 ± 0.59	39.0
Cu, %	9.66	4.22	4.01 ± 0.51	4.4
S, %	40.21	39.88	40.32 ± 0.29	39.2
N, %	3.19	3.17		3.1
C, %	10.94	10.88		11.5

[a] The compositions are calculated based on the ideal structural model, in which Ge occupies only adamantine clusters and Cu exclusively occupies M sites. [b] The calculation of composition is based on the M-site occupancy model obtained in this experiment and described in the text: $(Cu_{0.44}Ge_{0.56}S_{2.23})_4(Ge_4S_8)_3 \cdot 6(CH_3)_4N$. [c] EPMA: electron-probe microanalysis. See Table 1 for details.

2.28 Å rather than 2.34 Å. On the basis of these arguments, the unit cell contents of TMA-CuGS-2 can be expressed as a combination of adamantine and connection structural elements (Figures 1 and 3) in the following manner:

$[C_4H_{12}N]_{24}[(H_{0.06}Cu^{2+}_{4.32}Cu^{+}_{2.70}Ge_{8.99}S_{35.68})\text{-}(Ge_{48}S_{96})]$, where H is assumed for charge balance. They were not located in this structural study. This is close to the formulation $[C_4H_{12}N]_6[(Cu_{0.44}Ge_{0.56}S_{2.23})_4(Ge_4S_8)_3]$ without H atoms attached to framework, which is consistent with other open-framework sulfide structures.[1−6,8−14] However, this assignment is ambiguous and requires confirmation by anomalous scattering studies,[30] which are planned for the future.

Description of the Structure. The structure of TMA-CoMnGS-2, described in detail elsewhere,[7] closely resembles that of TMA-CuGS-2, save for the details of the M site. The framework is constructed from hexamers,[7] one hexamer consisting of two trimers, one left-hand and one right-hand (Figure 5a). The repeating of the hexamer forms a hexagonal column along the body-diagonal directions. Each column is surrounded by six similar columns, alternatively shifted $^1/_3a$ and $-^1/_3a$ relative to the center column (Figure 5b); a is the cubic unit cell parameter, 20.629 Å. The space between columns results in a set of trigonal channels along the body diagonals, about 6.2 Å on edge. The templating ion, TMA^+, does not reside at the intersection of these channels but rather lies close to their walls with its four $N-CH_3$ bonds approximately parallel to the four sets of channels as shown in Figure 5b.

In the TMA-MGS-2 structure, the M site is occupied by both Cu and Ge, accounting for the results of composition analysis by both EPMA and chemical methods. The M-site disorder, as evidenced by the splitting of M sites and the elongation of neighboring S atoms' displacement ellipsoids, results from the different stereochemical requirements of the Ge and Cu occupying these positions in the structure. This disorder also implies the TMA-CuGS-2 framework might support a variety of compositions, possibly determined by the starting materials and reaction conditions. One extreme case is that the M site is exclusively occupied by germanium. Reports of a phase,[1] termed TMA-GS-2 and with a diffraction pattern similar to that of TMA-CuGS-2 and TMA-CoMnGS-2, suggest this possibility has been realized. A structural analysis of this phase is of importance and will aid in understanding the crystal growth mechanism of these novel materials.

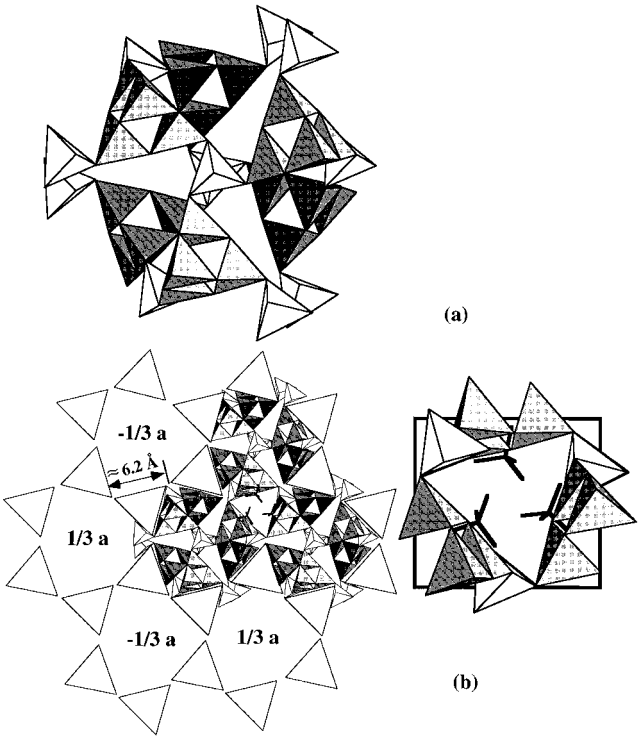

Figure 5. (a) Hexamer, consisting of a stack of a left-hand trimer (top) and a right-hand trimer (bottom) projected along [111]; (b) array of hexagonal-like columns projected along [111]. The shifts of surrounding columns relative to the center column are $^1/_3a$ or $-^1/_3a$ (a = 20.629 Å) as marked in the picture. The open triangles represent the channels running along [111]. The orientations of the organic templates within channels are shown on the right. Each TMA^+ cation has its four methyl groups oriented approximately parallel to each of the four intersecting channels.

Acknowledgment. We thank the National Science Foundation (DMR 94-13003) for financial support. We are grateful for the experimental assistance of M. Kunz, D. M. Nellis, C. Cahill, G. Symmes, and J. Rijssenbeek. Research carried out in part of the National Synchrotron Light Source at Brookhaven National Laboratory which is supported by the U.S. Department of Energy, Division of Materials Sciences and Division of Chemical Sciences. The SUNY X3 beamline at the NSLS is supported by the Division of Basic Energy Sciences of the U.S. Department of Energy (DE-FG02-86ER45231).

Supporting Information Available: Tables of anisotropic displacement and geometric parameters (1 page); table of observed and calculated structure factors (4 pages). Ordering information is given on any current masthead page.

CM950375X

(30) Coppens, P. *Synchrotron Radiation Crystallography*; Academic Press: New York, 1992.
(31) Johnson, C. K. *ORTEP*; ORNL Report 5138, Oak Ridge National Laboratory, Oak Ridge, TN, 1976.